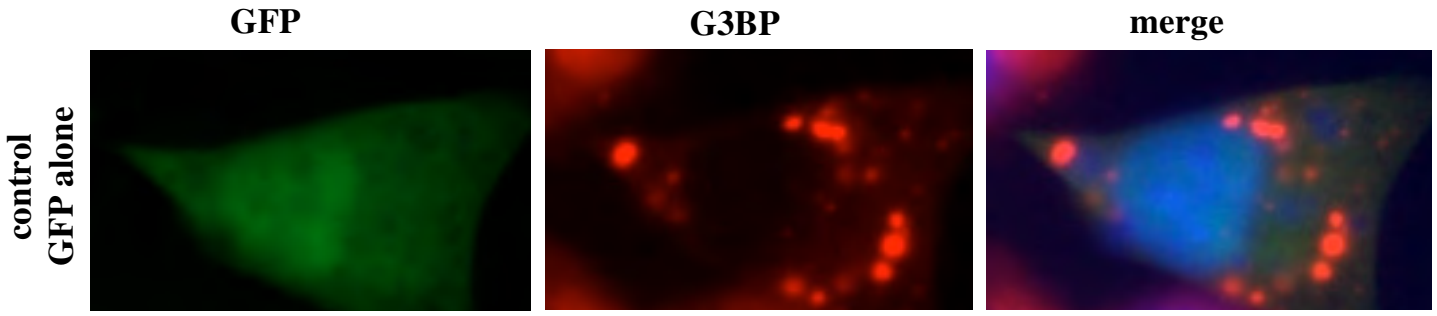

Fig. S1. GFP alone does not co-localize with G3BP in stressed NIH3T3 cells.

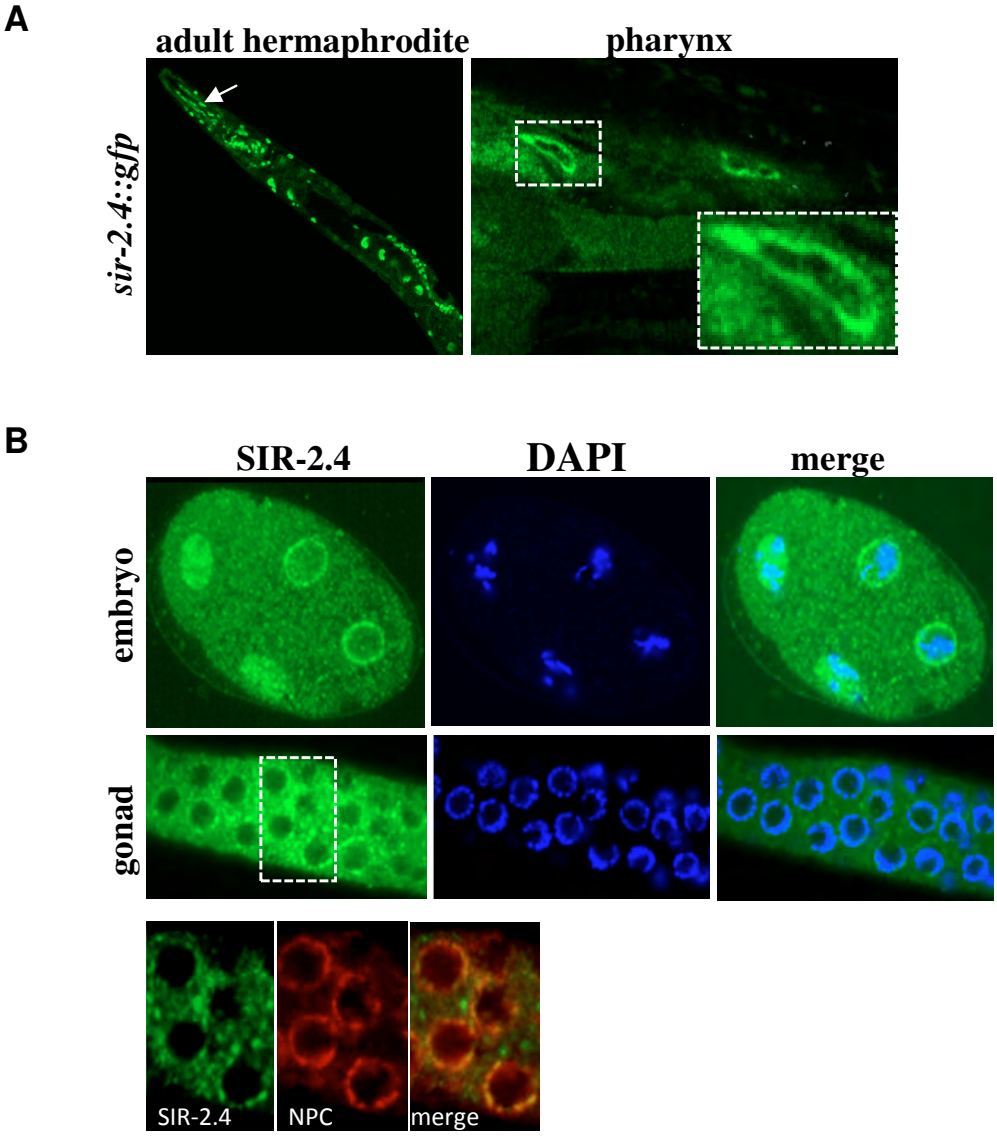

Fig. S2. SIR-2.4 is predominantly a nuclear envelope associated protein. (A, B) GFP-tagged SIR-2.4 protein (A) or endogenous SIR-2.4 is partially co-localized with nuclear pore complex (NPC) (B).

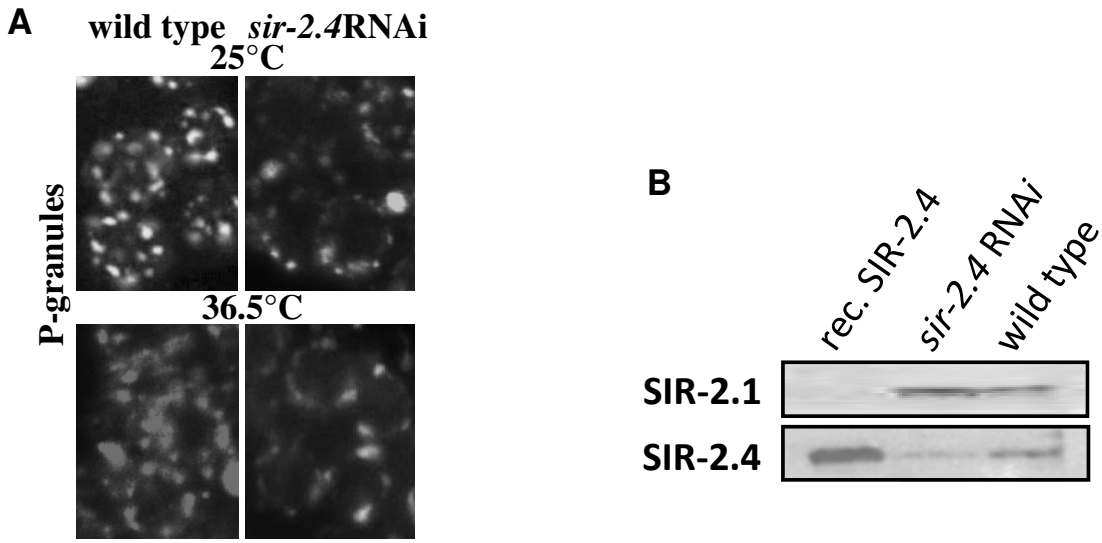

Fig. S3. SIR-2.4 influences number of P-granules**.** (A) Representative images of P-granules found in pachytene stage germline nuclei of wild type and *sir-2.4*-depleted 3-days old hermaphrodites at different temperatures. (B) Efficiency of *sir-2.4* knockdown. SIR-2.1 served as a loading control.

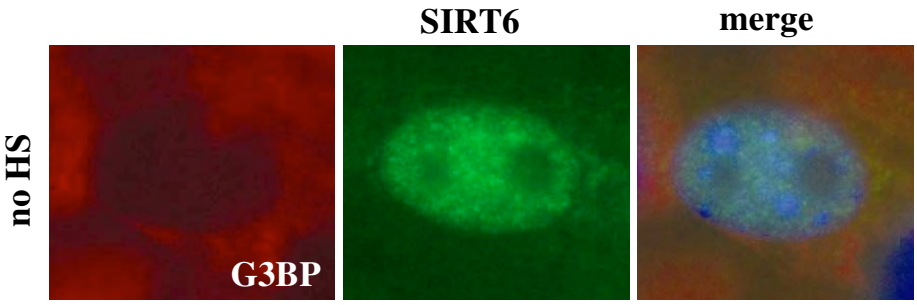

Fig. S4. Co-localization study of endogenous SIRT6 and G3BP in unstressed NIH3T3 cells.

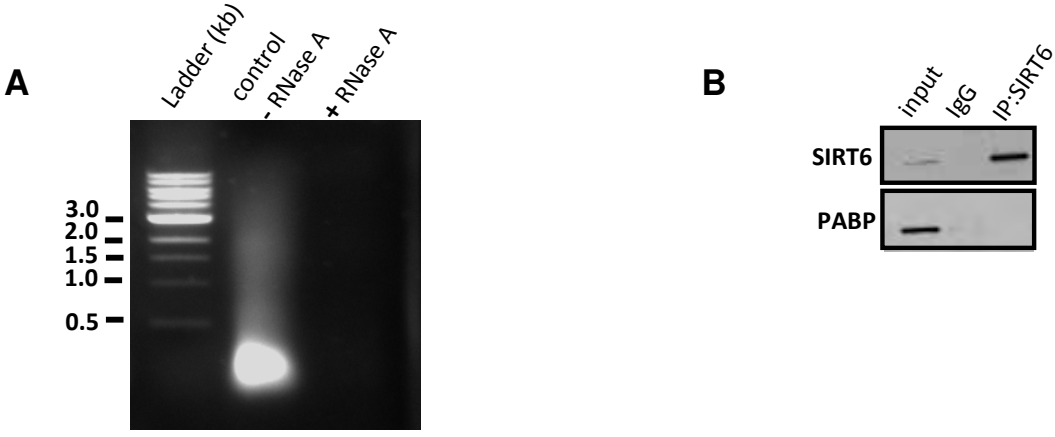

Fig. S5. (A) The effectiveness of RNAse treatment in lysates prior to the immunoprecipitation assessed on agarose gel. (B) SIRT6 does not bind to *in vitro* translated PABP1.

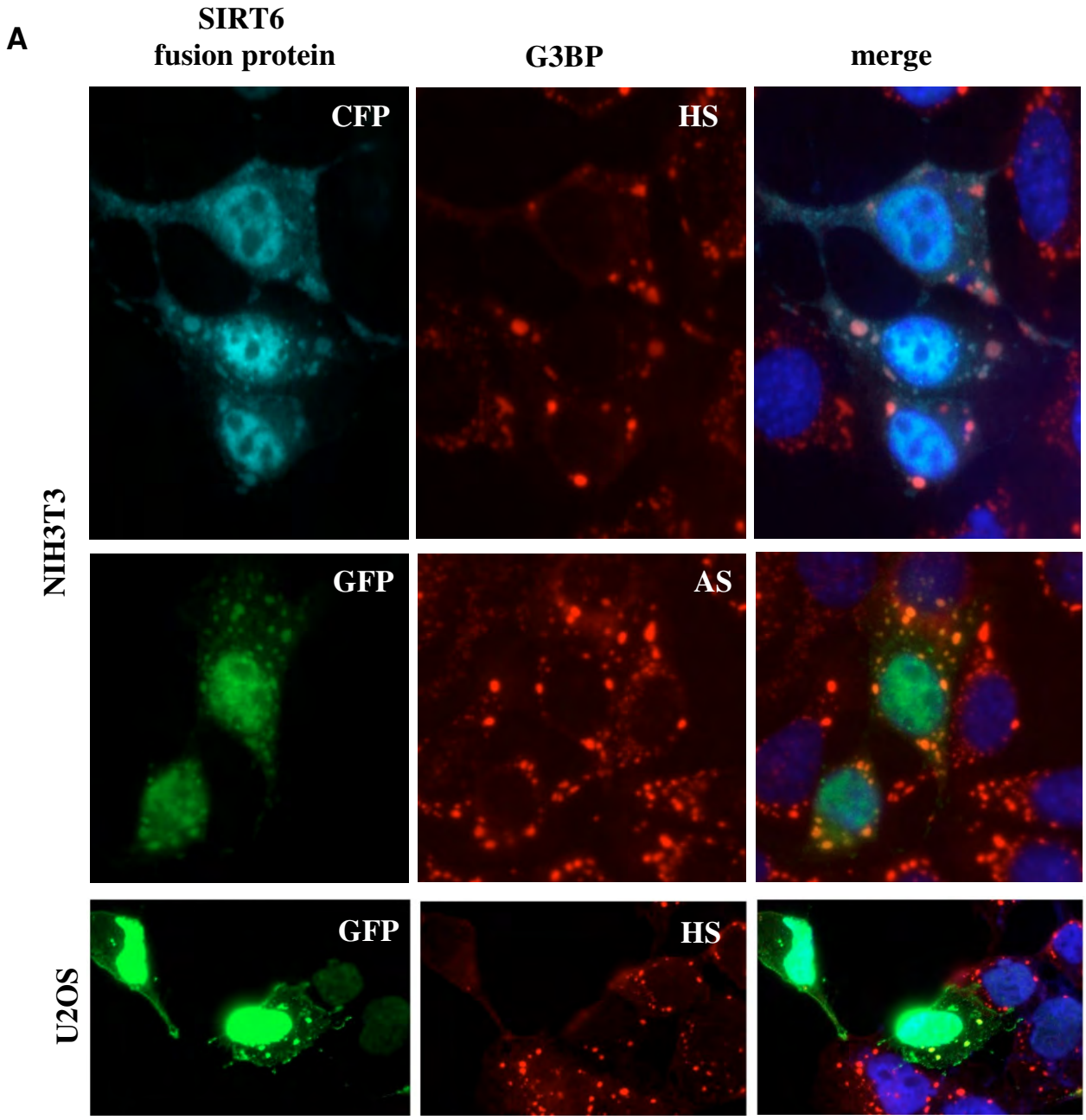

Fig. S6. SIRT6 localizes into SGs regardless of cell type or stress stimuli. (A) Co-localization study of CFP- or GFP-tagged SIRT6 protein with endogenous G3BP in stressed cells; HS for heat shock, AS for sodium arsenite.

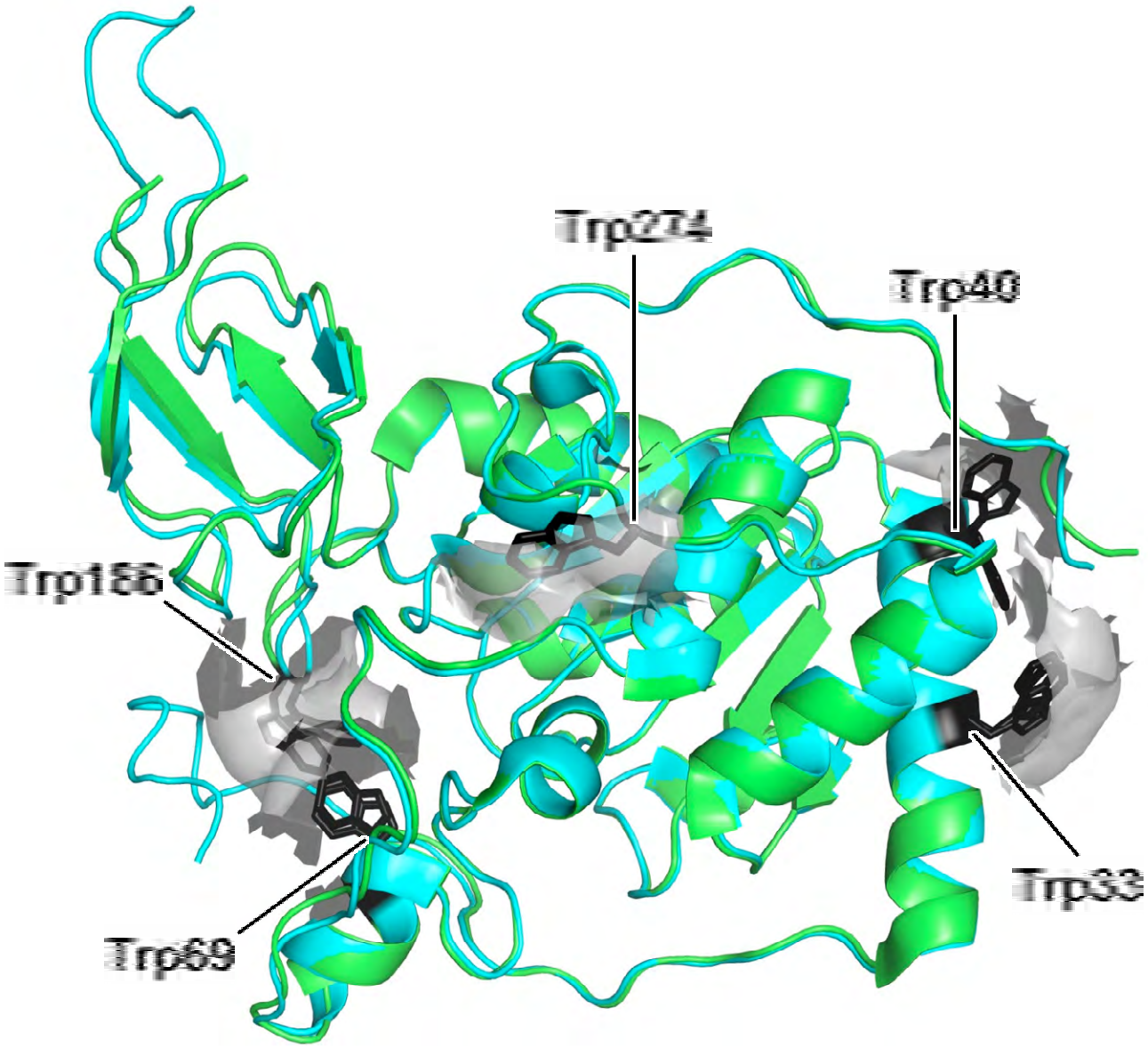

Fig. S7. Location of tryptophan residues in human SIRT6**.** Two crystal structures of human SIRT6 were globally aligned (PDB ID: 3K35, green & 3ZG6, cyan) with a root-mean-square deviation of 0.280 Å. Sidechains of tryptophan residues are shown in black with solvent-accessible surface in grey. Evidently, these residues except for Trp69 are located close to the protein surface. Molecular modeling and ray tracing were performed using Pymol (Schrödinger, LLC., USA).

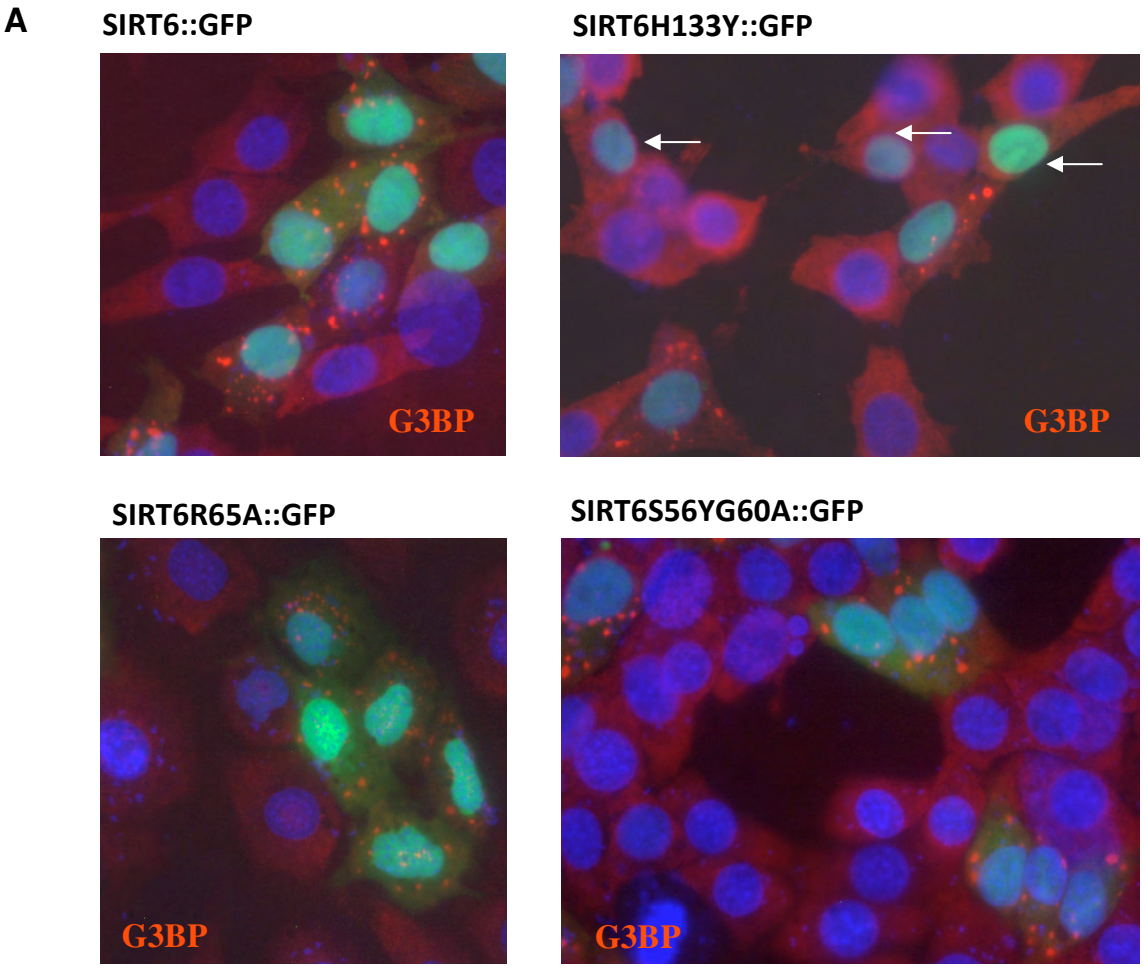

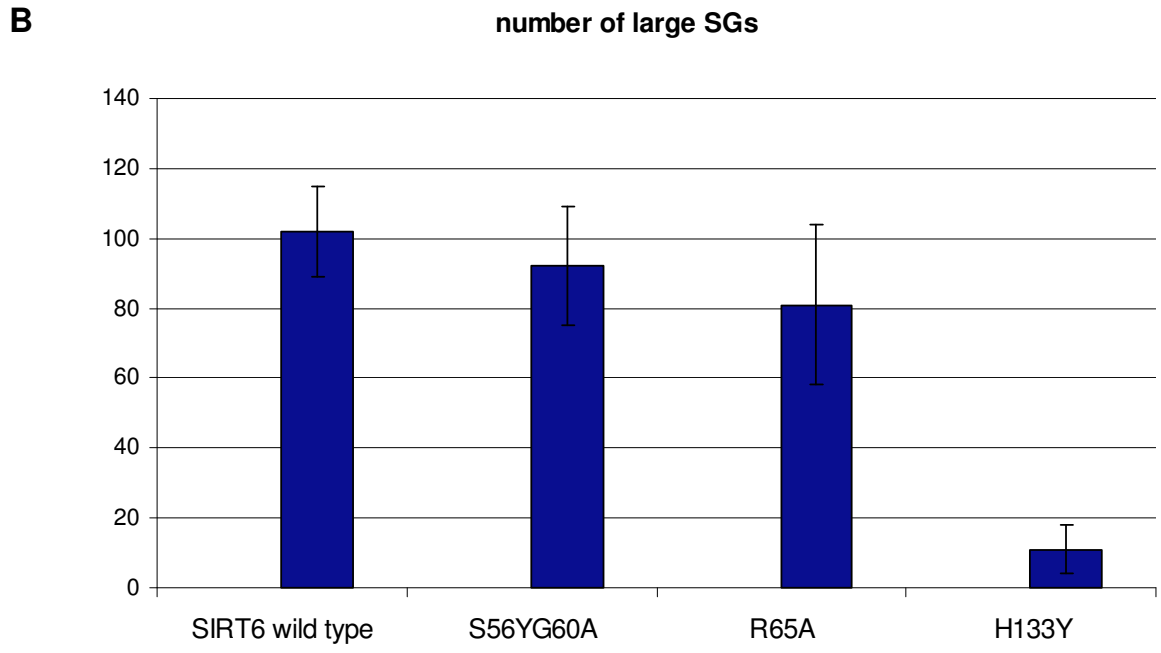

Fig. S8. (A) SIRT6 enzymatic activity induces G3BP formation. NIH3T3 cells, transfected with SIRT6::GFP and SIRT6::GFP constructs carrying point mutations, were fixed, stained with anti-G3BP antibody (red) without heat shock and analyzed for the presence of the G3BP stress granules. Arrows point at transfected cells with SIRT6H133Y plasmid (green fluorescence) without G3BP granules. (B) The graph shows the average size of G3BP granules. Analysis was based on 50 transfected cells. The large class of granules was identified on the basis of size (large - 31-230 pixels^2). Results shown are mean values of three independent experiments, error bars, mean ± s.d.

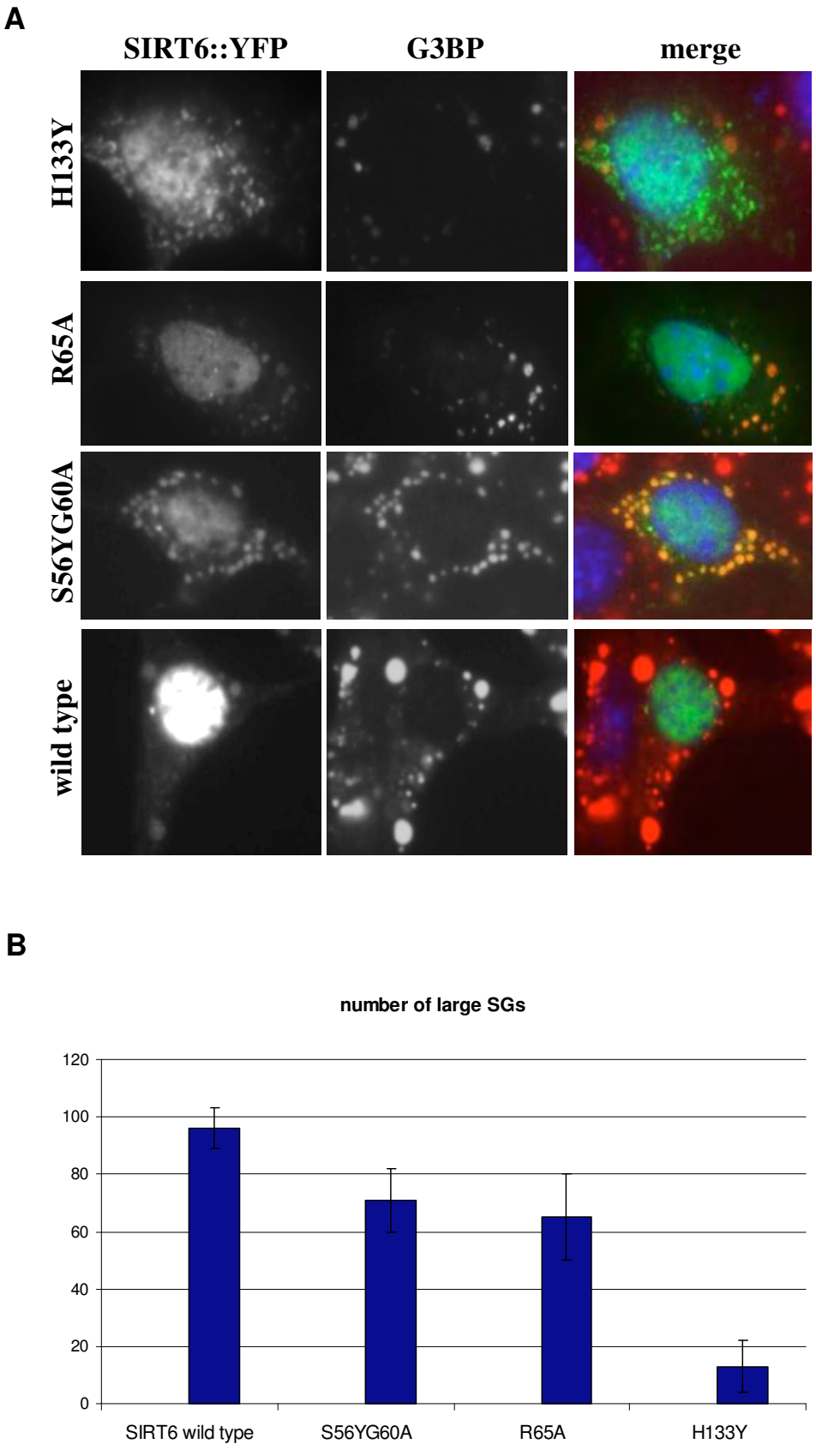

Fig. S9. (A) Deacetylase activity of SIRT6 influences the size of G3BP granules in stressed NIH3T3 cells. (A) Cells were transfected with SIRT6::GFP-point mutation constructs as indicated and analyzed 24 hours post-transfection for SGs formation using anti-G3BP antibody. (B) The graph shows the average size of SGs. Analysis was based on 50 transfected cells. The large class of granules was identified on the basis of size (large - 31-230 pixels^2). Results shown are mean values of three independent experiments, error bars, mean ± s.d.

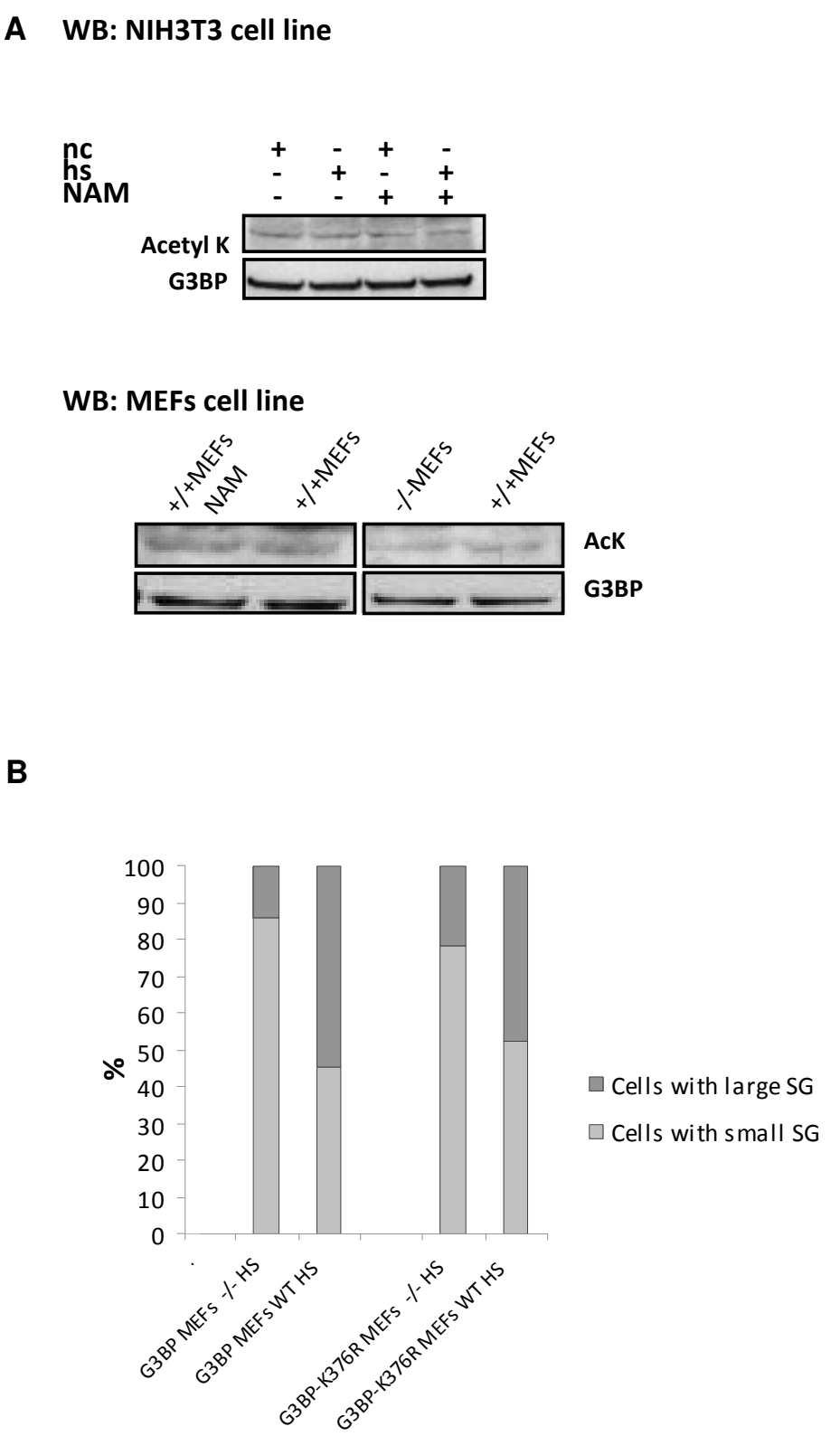

Fig. S10. SIRT6 does not influence the G3BP acetylation level. **(**A) Equal amounts of NIH3T3 or MEF cell lysates were analyzed on western blot. Deficiency of SIRT6 did not influence the acetylation level of G3BP. AcK for anti-acetylated lysine antibody; NAM for nicotinamide; nc for normal condition; hs for heat shock condition. (B) The graph represents the G3BP foci formation regarding the presence or absence of acetylation site at lysine 376.

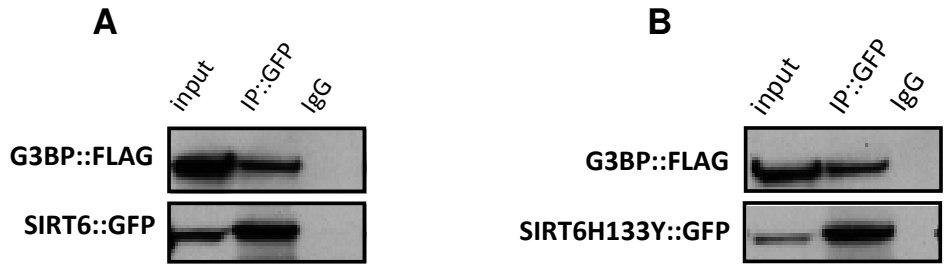

Fig. S11. SIRT6-G3BP association does not depend on SIRT6 enzymatic activity. (A, B) Western blot analysis showing co-immunoprecipitation of the SIRT6 wild type fusion protein (A) and catalytic-mutant SIRT6 (B) with G3BP.

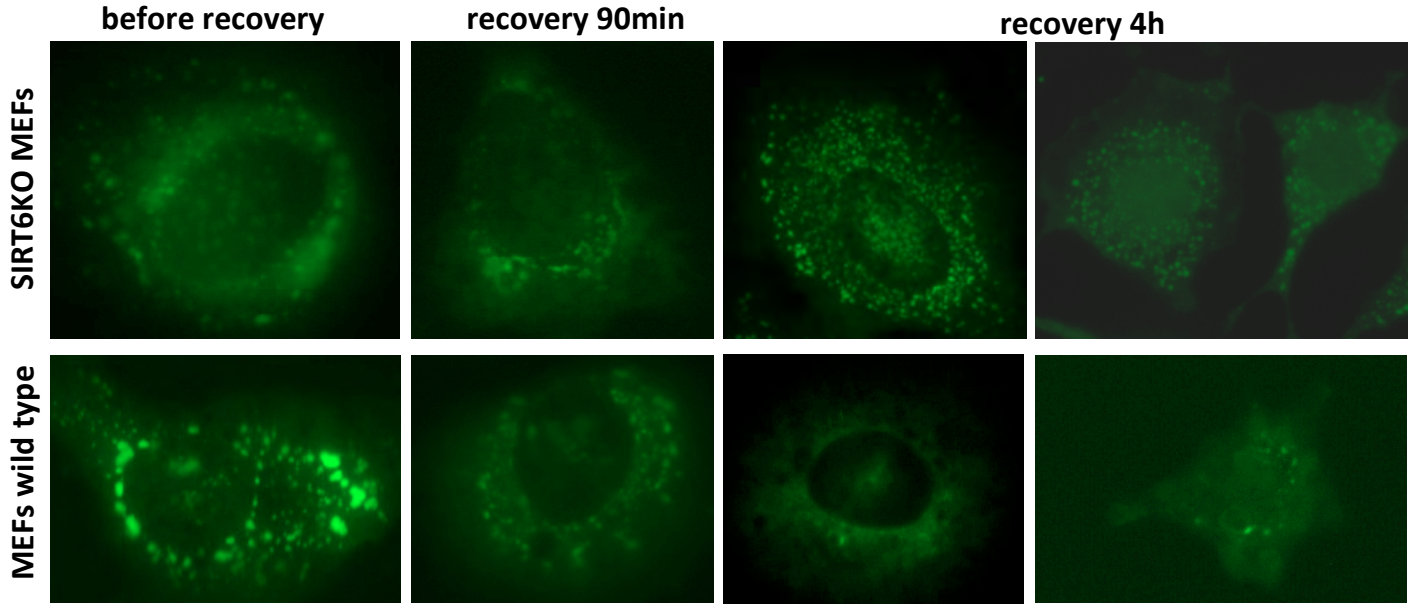

Fig. S12. SIRT6 impacts G3BP assembly. Representative images of stress granules in wild type (SIRT6+/+) and knockout (SIRT6-/-) MEFs cells. Both cell lines were transfected with G3BP::GFP, heat shock-treated and than incubated at 37°C. Finally, the cells were monitored for the size of stress granules before and after recovery by fluorescence microscopy.